



# Activation of peroxymonosulfate on visible light irradiated TiO<sub>2</sub> via a charge transfer complex path



Yoosang Jo<sup>a,1</sup>, Chuhyung Kim<sup>a,1</sup>, Gun-Hee Moon<sup>a</sup>, Jaesang Lee<sup>b,\*</sup>, Taicheng An<sup>c</sup>, Wonyong Choi<sup>a,c,\*</sup>

<sup>a</sup> Department of Chemical Engineering and Division of Environmental Science and Engineering, Pohang University of Science and Technology (POSTECH), Pohang 37673, Republic of Korea

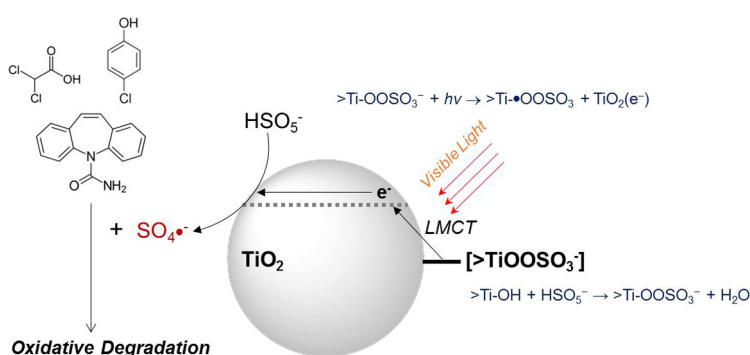
<sup>b</sup> Civil, Environmental, and Architectural Engineering, Korea University, Seoul 136-701, Republic of Korea

<sup>c</sup> Guangzhou Key Laboratory of Environmental Catalysis and Pollution Control, Institute of Environmental Health and Pollution Control, School of Environmental Science and Engineering, Guangdong University of Technology, Guangzhou 510006, Guangdong, China

## HIGHLIGHTS

- PMS serves as a complexing ligand and a radical precursor in the activation process.
- Visible light irradiation activates PMS on TiO<sub>2</sub> via ligand-to-metal charge transfer.
- The TiO<sub>2</sub>/PMS/visible light system shows catalytic performance in organic oxidation.

## GRAPHICAL ABSTRACT



## ARTICLE INFO

### Keywords:

Peroxymonosulfate activation  
Visible light  
Surface complex  
Ligand-to-metal charge transfer (LMCT)  
Sulfate radical  
Advanced oxidation process (AOP)

## ABSTRACT

Photo-induced activation of peroxymonosulfate (PMS) has been enabled by either the direct photolysis of the peroxide bond or the semiconductor bandgap-excited photocatalysis. Whereas the existing approaches utilize UV light, this study first studied the utilization of visible light for the PMS activation in which the dual roles of PMS as a complexing ligand on TiO<sub>2</sub> and a precursor of sulfate radical (SO<sub>4</sub><sup>·-</sup>) are enabled via ligand-to-metal charge transfer (LMCT) mechanism. In this LMCT-mediated photocatalysis, PMS coordinated to TiO<sub>2</sub> as a surface complex is photoexcited by visible light to inject electrons to the CB of TiO<sub>2</sub>, which subsequently activate PMS to yield SO<sub>4</sub><sup>·-</sup>. Despite the lack of visible light activity of both TiO<sub>2</sub> and PMS, the addition of PMS induced a significant degradation of 4-chlorophenol and dichloroacetate on TiO<sub>2</sub> under visible light irradiation. Together with several spectroscopic analyses, the result revealed the formation of an interfacial charge transfer (CT) complex of PMS on TiO<sub>2</sub> and the LMCT-mediated PMS conversion into SO<sub>4</sub><sup>·-</sup>. Multi-activity assessment showed that the oxidizing capacity of TiO<sub>2</sub>/PMS varied depending on the substrate type; benzoic acid and acetaminophen were rapidly decomposed whereas nitrophenol oxidation was insignificant. The role of SO<sub>4</sub><sup>·-</sup> as the main oxidant was identified based on (1) quenching effect of methanol as a radical quencher, (2) coumarin

\* Corresponding authors at: Department of Chemical Engineering and Division of Environmental Science and Engineering, Pohang University of Science and Technology (POSTECH), Pohang 37673, Republic of Korea (W. Choi) and Civil, Environmental, and Architectural Engineering, Korea University, Seoul 136-701, Republic of Korea (J. Lee).

E-mail addresses: [lee39@korea.ac.kr](mailto:lee39@korea.ac.kr) (J. Lee), [wchoi@postech.edu](mailto:wchoi@postech.edu) (W. Choi).

<sup>1</sup> Both authors contributed equally to this work.

hydroxylation as an indication of  $\text{SO}_4^{\cdot-}$  formation, and (3) EPR spin-trapping technique. The comparison of  $\text{TiO}_2/\text{PMS}$  versus  $\text{Co}_3\text{O}_4/\text{PMS}$  suggested that the repeated acetaminophen decay was achievable with  $\text{TiO}_2/\text{PMS}$  without the loss of activating capacity whereas a gradual reduction in degradation efficiency was observed with  $\text{Co}_3\text{O}_4/\text{PMS}$ .

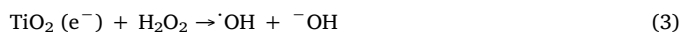
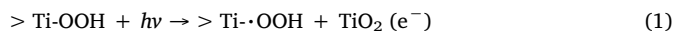
## 1. Introduction

Persulfate (collectively representing peroxymonosulfate (PMS;  $\text{HSO}_5^-$ ) and peroxydisulfate (PDS;  $\text{S}_2\text{O}_8^{2-}$ )) activation has been demonstrated to rapidly degrade a wide range of organic pollutants possessing different chemical structures through the production of sulfate radical ( $\text{SO}_4^{\cdot-}$ ) as a highly reactive intermediate ( $E^0(\text{SO}_4^{\cdot-}/\text{SO}_4^{2-}) = +2.5 - 3.1 \text{ V}_{\text{NHE}}$  [11] [2,3]). Compared with hydroxyl radical ( $\cdot\text{OH}$ ) ( $E^0(\cdot\text{OH}/\text{OH}^-) = +1.8 - 2.7 \text{ V}_{\text{NHE}}$  [4]), persulfate activation processes possibly outperform the conventional advanced oxidation processes (AOPs) utilizing  $\text{H}_2\text{O}_2$  in oxidation of recalcitrant organics; selected pollutants such as perfluorinated compounds and cyanuric acid that resist  $\cdot\text{OH}$ -induced oxidation could be degraded by  $\text{SO}_4^{\cdot-}$  [5,6]. The strategies to activate persulfate are based on the peroxide bond cleavage via energy and electron transfer processes; one-electron reduction of PMS readily takes place upon the addition of various transition metal-based reagents, leading to the conversion into  $\text{SO}_4^{\cdot-}$  (e.g.,  $\text{Co}^{2+} + \text{HSO}_5^- \rightarrow \text{Co}^{3+} + \text{SO}_4^{\cdot-} + \text{OH}^-$ ) [7,8]. Ferrous ion, electrochemically supplied from the sacrificial iron anode, can serve as a persulfate activator and a precursor of iron-based coagulant to effectively remove persistent organics (e.g., pentachlorophenol) [9,10]. Persulfate activation can be also initiated by  $\gamma$ -radiolysis [11], sonolysis [12], and electrolysis [13]. Since the homolytic scission of the PDS peroxide bond proceeds with elevating temperature above ca.  $30^\circ\text{C}$  [14], microwave radiation initiates  $\text{SO}_4^{\cdot-}$ -induced oxidation of organics in the presence of PDS [15]. The delivery of photon energy also enables persulfate activation; UV-C enables a direct photolysis of persulfate into  $\text{SO}_4^{\cdot-}$  [16] and semiconductor photocatalysts (e.g.,  $\text{TiO}_2$  [17], carbon nitride [18]) are photo-excited by UV-A or visible light to initiate persulfate reduction via conduction band (CB) electron transfer that leads to peroxide bond breakdown and subsequent  $\text{SO}_4^{\cdot-}$  production.

Due to the lack of visible light responsivity, reductive and oxidative transformation reactions of organic and inorganic pollutants by  $\text{TiO}_2$  are performed only with UV light. On the other hand, the use of adequate ligands forming surface charge-transfer (CT) complexes on  $\text{TiO}_2$  enables the redox reactions even under visible light irradiation; hydroxyl or carboxyl functional groups of selected compounds (e.g., phenol [19], EDTA [20], fullerol [21], and glucose [22]) undergo condensation reactions with surface hydroxyl groups on  $\text{TiO}_2$ , generating the visible-light-active CT complexes with the release of water molecules. The metal–ligand charge transfer (MLCT) process in which the excited CT complexes inject electrons to the CB of  $\text{TiO}_2$  allows the reductive treatment of some pollutants (e.g.,  $\text{CCl}_4$ ,  $\text{Cr(VI)}$ ) and production of hydrogen gas from water under visible light irradiation [23]. In particular, the electrons originated from the CT complexes are exploitable for the reduction of radical precursors such as  $\text{O}_2$  and  $\text{H}_2\text{O}_2$ , which likely leads to production of reactive oxygen species (ROS) and subsequent destruction of organic compounds [23]. This may lead us to consider the MLCT mechanism for activating persulfate via one-electron reduction under visible light illumination.

$\text{H}_2\text{O}_2$  forms a visible-light-responsive CT complex on  $\text{TiO}_2$  through the condensation reaction (i.e.,  $>\text{Ti-OH} + \text{H}_2\text{O}_2 \rightarrow >\text{Ti-OOH} + \text{H}_2\text{O}$ ) based on the FT-IR absorption band characteristic of surface hydroperoxy group (i.e., Ti- $\mu$ -peroxide; Ti-OOH) in the range of  $740\text{--}800 \text{ cm}^{-1}$  [24]. The surface complexation extends the absorption and photo-response of  $\text{TiO}_2$  up to  $550 \text{ nm}$  [23]. When exciting the CT complex with visible light, surface-bound Ti-peroxy radical forms as a short-lived oxidation intermediate with injecting an electron to  $\text{TiO}_2$  CB

(Eq. (1)). The peroxy radical further decomposes into tianol group and oxygen molecule (Eq. (2)), and the transferred electron reductively cleaves surface-absorbed  $\text{H}_2\text{O}_2$  into  $\cdot\text{OH}$  (Eq. (3)).



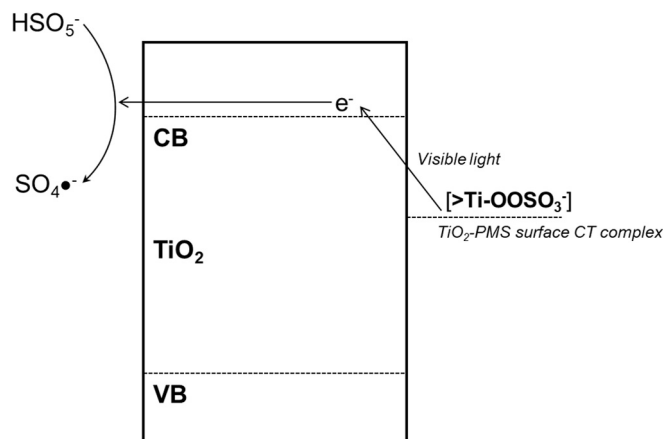
Considering the aforementioned photochemistry of the  $\text{TiO}_2\text{-H}_2\text{O}_2$  surface CT complex [25], PMS as a simple peroxide is likely to serve the identical dual roles as a ligand and a radical precursor when the binary mixture of  $\text{TiO}_2$  and PMS is exposed to visible light (see Scheme 1); PMS contains a hydroxyl moiety to allow the surface complexation on  $\text{TiO}_2$ , and the electrons transferred from the visible-light-excited CT complexes possibly cause the production of PMS-derived radical (i.e.,  $\text{SO}_4^{\cdot-}$ ).

In this study, the  $\text{TiO}_2\text{-PMS}$  CT complex-mediated activation of PMS (i.e., conversion of PMS to  $\text{SO}_4^{\cdot-}$ ) for the oxidative degradation of various organic pollutants under visible light irradiation was first hypothesized and then validated. The surface complexation was confirmed by spectroscopic characterizations. The effects of reaction parameters such as pH, PMS concentration, and irradiation wavelengths were investigated and the mechanism of PMS activation under visible light was proposed based on various experimental evidences.

## 2. Material and methods

### 2.1. Chemicals and materials

The chemicals that were used as-received in this study include the following: titanium dioxide ( $\text{TiO}_2$ , Degussa P25, average surface area =  $50 \text{ m}^2/\text{g}$ , particle size =  $20\text{--}30 \text{ nm}$ ), cobalt oxide ( $\text{Co}_3\text{O}_4$ , Aldrich), acetaminophen (Aldrich), carbamazepine (Aldrich), 4-chlorophenol (4-CP, Aldrich), furfuryl alcohol (Aldrich), nitrobenzene (Aldrich), nitrophenol (Aldrich), phenol (Junsei), sodium dichloroacetate (DCA, Aldrich), potassium peroxymonosulfate (OXONE, PMS, Aldrich), lithium perchlorate (Aldrich), sodium chloride (Aldrich), sodium sulfate (Aldrich), iodic acid (Aldrich), sodium fluoride (Aldrich), methanol (J.T. Baker), *tert*-butyl alcohol (Aldrich),



**Scheme 1.** Proposed mechanism for PMS activation through visible light-induced charge transfer in  $\text{TiO}_2\text{-PMS}$  surface complex.

sodium dichromate dihydrate (Aldrich), phosphoric acid (Aldrich), coumarin (Aldrich), 2,2'-azino-bis(3-ethylbenzothiazoline-6-sulfonic acid) diammonium salt (ABTS, Aldrich), 5,5-dimethyl-1-pyrroline N-oxide (DMPO, Tokyo Chemical Industry CO. Ltd.), sodium tetraborate (Aldrich), potassium hydrogen phthalate (Aldrich), sodium phosphate monobasic (Aldrich), sodium phosphate dibasic (Aldrich), hydrochloric acid (Samchun), sodium hydroxide (Aldrich), perchloric acid (Aldrich), sodium bicarbonate (Kanto Chemical), sodium carbonate (Junsei), phosphoric acid (Aldrich), and acetonitrile (J.T Baker). All chemicals used in this study were of the highest purity available and used without further purification. Ultrapure water ( $> 18 \text{ M}\Omega\text{-cm}$ ) produced by a Barnstead purification system was used to prepare all the suspensions and solutions.

## 2.2. Catalyst modification and characterization

The adsorption of PMS on  $\text{TiO}_2$  surface is critically required for the activation and it can be inhibited by adsorbing phosphate on  $\text{TiO}_2$  surface. When the effect of surface passivation by phosphate was investigated,  $\text{TiO}_2$  was modified as follows. 0.1 g  $\text{TiO}_2$  was suspended in 100 mL aqueous solution of 100 mM phosphoric acid and continuous stirring for 5 h allowed phosphate anions to be sufficiently adsorbed on  $\text{TiO}_2$  surface. The resultant powder (noted as P- $\text{TiO}_2$ ) was dried in an oven at  $80^\circ\text{C}$  for 2 h, subjected to thermal treatment in a furnace at  $300^\circ\text{C}$  for 1 h, and washed with distilled water to remove weakly-bound phosphate anions. Electron energy loss spectroscopy (EELS) mapping analysis was performed using a JEM-2200FS microscope with Cs correction to confirm the uniform distribution of sulfur on the  $\text{TiO}_2/\text{PMS}$  and P- $\text{TiO}_2/\text{PMS}$  samples. The surface composition of  $\text{TiO}_2$  adsorbed with PMS was investigated by X-ray photoelectron spectroscopy (XPS, ESCALAB 250, VG Scientific) using the Al  $K\alpha$  line (1486.6 eV) as an excitation source. To identify the surface functional groups on the  $\text{TiO}_2/\text{PMS}$  and P- $\text{TiO}_2/\text{PMS}$  samples, the infrared spectra were acquired with a Thermo Scientific iS50 Fourier transform infrared (FT-IR) spectrometer in a reflectance mode. Diffuse reflectance UV–visible absorption spectra of pure  $\text{TiO}_2$ , P- $\text{TiO}_2$ , P- $\text{TiO}_2/\text{PMS}$ , and  $\text{TiO}_2/\text{PMS}$  were recorded with a UV/visible spectrophotometer (Shimadzu UV-2600) to monitor the possible red-shift of the absorption edge of  $\text{TiO}_2/\text{PMS}$  in the visible light region.

## 2.3. Experimental procedure and analytical methods

The photodegradation of organic compounds proceeded in a

magnetically-stirred 50 mL Pyrex reactor under air-equilibrated condition. The reactor was irradiated with a 300-W Xe-arc lamp (Oriel). The incoming light passed through 10 cm IR filter to minimize temperature increase during the photo-illumination, and a cut-off filter allowing  $\lambda > 420 \text{ nm}$  was used for visible light irradiation. Typical experimental suspensions contained 0.5 g/L  $\text{TiO}_2$ , 0.5 mM PMS, and 0.1 mM target substrate, and the pH of the aqueous suspensions was adjusted to ca. 5.0 with concentrated  $\text{HClO}_4$  or  $\text{NaOH}$ . Prior to the photo-irradiation, the suspensions were agitated in the dark for 30 min in order to make sure that the removal of organic substrate via sorption was negligible. Aliquots of 1 mL were withdrawn from the suspensions at pre-determined time intervals, filtered through a  $0.45\text{-}\mu\text{m}$  PTFE syringe filter (Millipore), and injected to a 2-mL amber glass vial.

Residual concentrations of most organic substrates were measured using a high performance liquid chromatography (HPLC, Agilent 1260 Infinity) equipped with a diode array detector and a ZORBAX 300SB-C18 column ( $4.6 \text{ mm} \times 150 \text{ mm}$ ). The binary mixture consisting of 0.1% of aqueous phosphoric acid and acetonitrile (80:20 v/v) was used as a mobile phase. Dichloroacetate (DCA) and chloride ion were quantified with an ion chromatograph (IC, Dionex DX-120) equipped with a Dionex Ionpac AS-14 column and a conductivity detector. The eluent comprised 3.5 mM  $\text{Na}_2\text{CO}_3$  and 1 mM  $\text{NaHCO}_3$ . PMS concentration was monitored according to modified ABTS method [26]; product formed through the one-electron oxidation of ABTS was colorimetrically determined at 415 nm. Hydroxylation of coumarin (leading to the production of 7-hydroxycoumarin) was employed as an indirect indication of  $\text{SO}_4^{\cdot-}$  yield [27]; the oxidation product was monitored by a spectrofluorometer (HORIBA, Fluoromax 4C-TCSPC) with the excitation wavelength at 332 nm and emission wavelength monitored at 450 nm. For electron paramagnetic resonance (EPR) analysis, 5,5-dimethyl-1-pyrroline-N-oxide (DMPO) was employed as a spin-trapping agent for  $\text{SO}_4^{\cdot-}$ . The EPR spectra was recorded for the samples of  $\text{TiO}_2$ , PMS, and the binary mixture of  $\text{TiO}_2$  and PMS using a JES-TE 300 spectrometer (JEOL, Japan) under the following conditions: microwave power = 3 mW, microwave frequency = 9.42 GHz, center field = 338.25 mT, modulation width = 0.2 mT, and modulation frequency = 100 kHz.

Photocurrent measurement was conducted in a conventional three-electrode cell using a computer-controlled potentiostat (Gamry, Reference 600). The electrochemical cell magnetically stirred and continuously purged with argon to maintain an anoxic condition. The cell contained a  $\text{TiO}_2$ -coated fluorine-doped tin oxide (FTO) glass (i.e.,  $\text{TiO}_2/\text{FTO}$ ) was prepared using doctor-blade method as described

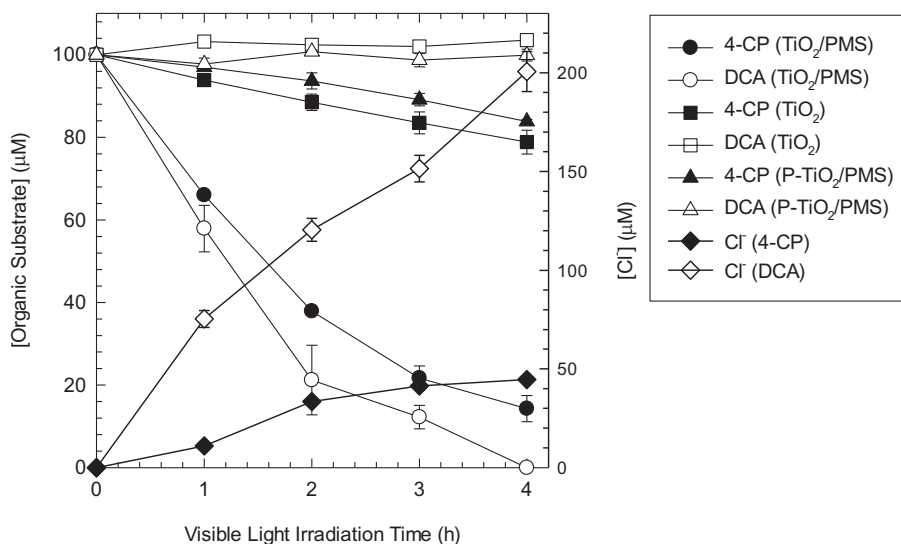


Fig. 1. Oxidative degradation of 4-chlorophenol (4-CP) and dichloroacetate (DCA) in the suspension of  $\text{TiO}_2$  and PMS under visible light. P- $\text{TiO}_2$  indicates  $\text{TiO}_2$  whose surface is adsorbed with phosphate ions. ( $[\text{TiO}_2]_0 = 0.5 \text{ g/L}$ ;  $[\text{PMS}]_0 = 0.5 \text{ mM}$ ;  $[\text{4-CP}]_0 = [\text{DCA}]_0 = 100 \text{ }\mu\text{M}$ ;  $\text{pH}_i = 5.0$ ).

previously [28]), a Pt wire, and a Ag/AgCl (3.0 M KCl) electrode as the working, counter, and reference electrode, respectively, in 10 mM LiClO<sub>4</sub> electrolyte solution. For photocurrent monitoring, the working electrode was biased at an applied potential of +1.0 V (vs Ag/AgCl). A 300-W Xe-arc lamp equipped with an optical filter cutting off below 455 nm was used as a light source.

### 3. Results and discussion

#### 3.1. Visible-light-induced oxidation of organic pollutants by TiO<sub>2</sub>/PMS

Fig. 1 shows that 4-CP degradation significantly proceeded with the concurrent release of chloride ions (Cl<sup>-</sup>) in the aqueous TiO<sub>2</sub> suspensions containing PMS under visible light irradiation. It is noted that the generated chloride concentration was lower than the removed 4-CP concentration, which implies that the mineralization was not complete. The TOC (total organic carbon) measurement demonstrated that ca. 80% of initial TOC was mineralized after visible light illumination for 20 h in the TiO<sub>2</sub>/PMS/4-CP system (Fig. S1), which indicates that the mineralization proceeds at a much slower rate. The possible involvement of SO<sub>4</sub><sup>·-</sup> as an oxidant should enable the oxidative conversion of organics into CO<sub>2</sub> [29]. The observation of the visible light-induced degradation and mineralization of 4-CP appears to contradict the fact that TiO<sub>2</sub> is inactive to visible light. Direct photolysis of PMS with visible light caused no reduction in 4-CP concentration, and the binary mixture of TiO<sub>2</sub> and PMS did not remove any detectable amount of 4-CP in the dark (Fig. S2). About 20% of 4-CP was degraded in the visible light irradiated TiO<sub>2</sub> suspension even when PMS was absent, which likely results from the formation of interfacial CT complexes of 4-CP on TiO<sub>2</sub> surface; surface-complexed phenols are readily excited by visible light to decompose oxidatively by injecting electrons to the CB of TiO<sub>2</sub> [19]. However, considering that almost threefold faster 4-CP decay was achieved with TiO<sub>2</sub>/PMS under visible light irradiation, the results here may reveal the possibilities of 1) formation of a visible-light-absorbing CT complex of PMS on TiO<sub>2</sub> and 2) SO<sub>4</sub><sup>·-</sup> production via the LMCT mechanism in which the surface complexed PMS undergoes photo-excitation followed by one-electron reduction (see Scheme 1). Contrary to the previous finding on visible-light-driven H<sub>2</sub>O<sub>2</sub> activation via LMCT [24], we observed that 4-CP oxidation was not markedly enhanced when H<sub>2</sub>O<sub>2</sub> was applied instead of PMS (Fig. S3).

The dual roles of PMS as a surface complexing agent and a radical precursor became more pronounced when DCA was used as an alternative substrate; DCA itself cannot form a CT complex with TiO<sub>2</sub>, unlike phenolic compounds. With the stoichiometric evolution of Cl<sup>-</sup>, DCA completely decomposed after 4-h visible light irradiation in the aqueous TiO<sub>2</sub>/PMS suspension (Fig. 1). Neither photolysis of PMS nor dark adsorption by the TiO<sub>2</sub>/PMS mixture removed DCA (Fig. S2). Whereas TiO<sub>2</sub> alone caused the noticeable 4-CP oxidation with visible light, DCA was not degraded at all (Fig. 1), which confirmed the inability of DCA to form a surface CT complex on TiO<sub>2</sub>. PMS decomposition proceeded at a similar rate in the visible light-irradiated TiO<sub>2</sub> suspension in the presence and absence of organic substrates (Fig. S4). The results collectively rule out a possibility that surface complexation between TiO<sub>2</sub> and organic substrate (i.e., 4-CP) followed by the charge transfer under visible light irradiation is responsible for the reductive conversion of PMS to SO<sub>4</sub><sup>·-</sup>. This indicates the possible involvement of a surface CT complex between PMS and TiO<sub>2</sub> in the LMCT mechanism (note that H<sub>2</sub>O<sub>2</sub> as a simple peroxide forms visible light responsive complex on TiO<sub>2</sub> surface [25]). TiO<sub>2</sub> adsorbed with phosphate ions (noted as P-TiO<sub>2</sub>) drastically retarded the degradation of both target substrate (i.e., 4-CP and DCA) and PMS decomposition in the TiO<sub>2</sub>/PMS/visible light system (Figs. 1 and S4). Phosphates are well known to be strongly anchored onto TiO<sub>2</sub> surface to hinder the adsorption of other substrates [30]. This result also assures the role of PMS as the surface complexing ligand.

The TiO<sub>2</sub>/PMS system was examined for the oxidative degradation of various organic pollutants including acetaminophen, benzoic acid, carbamazepine, furfuryl alcohol, nitrobenzene, nitrophenol, and phenol (Fig. 2).

Degradation efficiency depends on the type of substrate. Benzoic acid and carbamazepine were rapidly decomposed, and acetaminophen, nitrobenzene, and phenol were degraded at moderate rates, while nitrophenol and furfuryl alcohol underwent relatively slow decay. The performance of TiO<sub>2</sub>/PMS in oxidative degradation appears to rely on the oxidizing capacity of SO<sub>4</sub><sup>·-</sup> rather than the coordination capability of the organic substrate as a ligand. For example, nitrophenol that should form a surface CT complex on TiO<sub>2</sub> through the phenolic functional group was actually less degraded than carbamazepine and nitrobenzene (Fig. 2). On the other hand, organic substrates that were more susceptible to oxidation on TiO<sub>2</sub>/PMS exhibit higher reactivity toward SO<sub>4</sub><sup>·-</sup>; benzoic acid rapidly reacts with SO<sub>4</sub><sup>·-</sup> ( $k(\text{benzoic acid} + \text{SO}_4^{\cdot-}) = 1.2 \times 10^9 \text{ M}^{-1} \text{ s}^{-1}$ ) whereas nitrobenzene is much less reactive toward SO<sub>4</sub><sup>·-</sup> ( $k(\text{nitrobenzene} + \text{SO}_4^{\cdot-}) < 10^6 \text{ M}^{-1} \text{ s}^{-1}$ ) [31]. Photochemically- or thermally-activated persulfate was demonstrated to effectively degrade carbamazepine [32,33].

#### 3.2. Formation of visible-light-absorbing surface complex

The EELS map of TiO<sub>2</sub> sample obtained after 5 min exposure to aqueous PMS solution shows that sulfur atoms are uniformly distributed on the TiO<sub>2</sub> surface (Fig. 3f), which is in marked contrast to the EELS image of pure TiO<sub>2</sub> in Fig. 3c. The XPS spectrum of S 2p in the PMS-treated TiO<sub>2</sub> also confirms the surface sulfur species (Fig. 3h) and the surface sulfur content was estimated to be ca. 2.8%. The FT-IR absorption band associated with S-O bond stretching was found at 1199 cm<sup>-1</sup> [34] and became more pronounced when applying 10-fold higher concentration of PMS (Fig. 3g), which corroborates the possible PMS linkage to the surface of TiO<sub>2</sub>. The IR band assignable to the stretching vibration of S-O group remained when the calcination temperature increased up to 500 °C, but further temperature elevation (i.e., 700 °C) eliminated the S-O stretching band (Fig. S5). This indicates that the TiO<sub>2</sub>-PMS surface complex is stable up to 500 °C. Whereas the hydroxyl group characterized by the broad absorption band centered at 3400 cm<sup>-1</sup> [35] was detected in the IR spectrum of PMS alone, the corresponding IR band disappeared in the spectrum of TiO<sub>2</sub>/PMS (Fig. 3g). This supports the possibility that the hydroxyl moiety of PMS is involved in the surface chelation process (Eq. (4)).

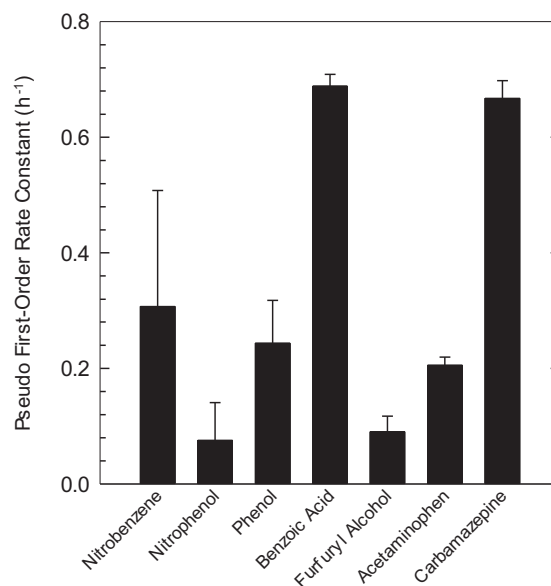
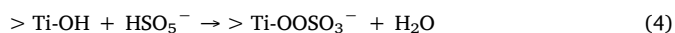
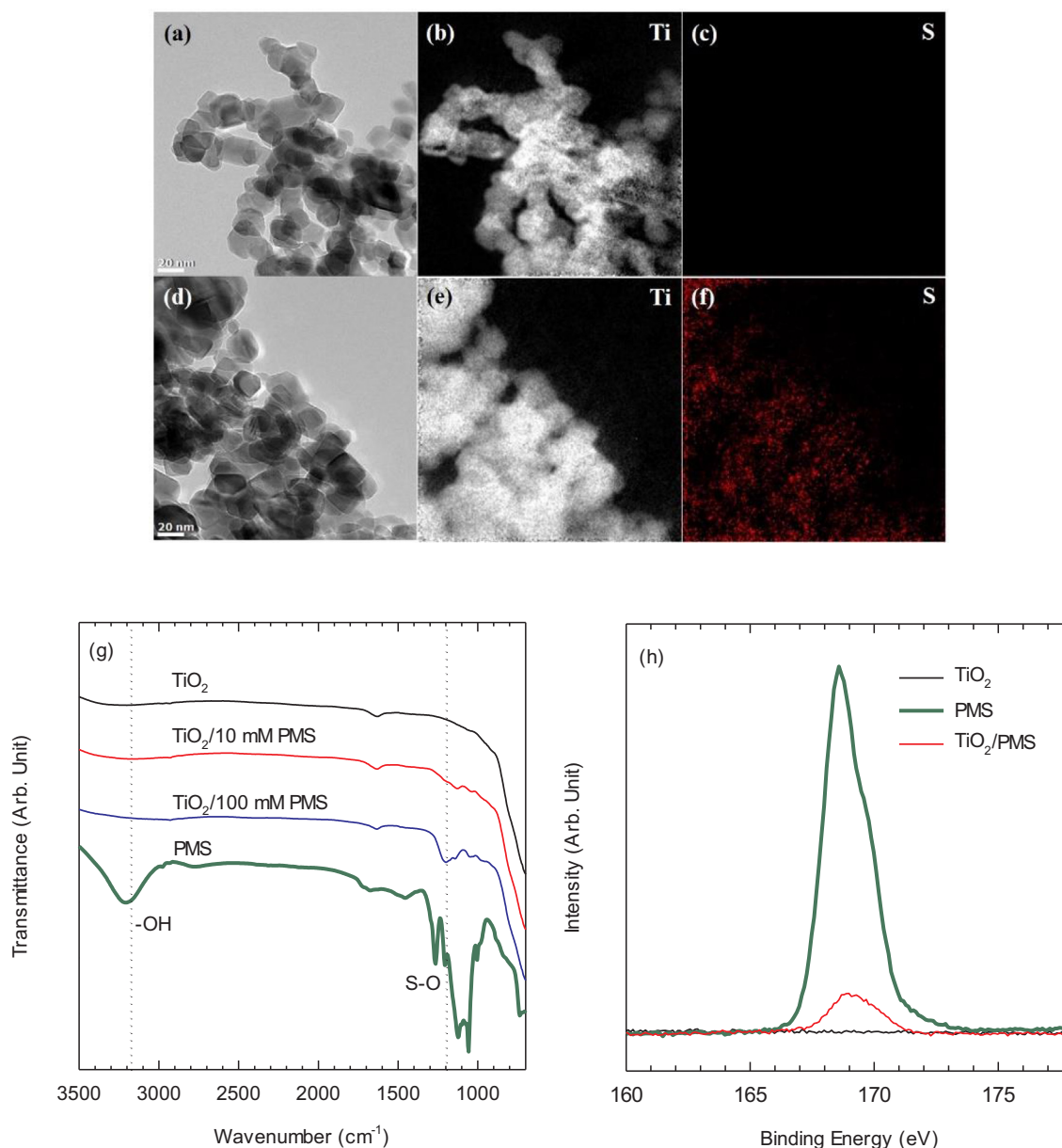


Fig. 2. Evaluation of TiO<sub>2</sub>/PMS activity for the visible-light-induced degradation of diverse organic compounds in terms of the photodegradation rate constant ([TiO<sub>2</sub>]<sub>0</sub> = 0.5 g/L; [PMS]<sub>0</sub> = 0.5 mM; pH<sub>i</sub> = 5.0; [organic compound]<sub>0</sub> = 100 μM, except [carbamazepine]<sub>0</sub> = 50 μM).



**Fig. 3.** (a) TEM image of pure TiO<sub>2</sub> with the corresponding EELS elemental mapping image of (b) Ti and (c) S, (d) TEM image of TiO<sub>2</sub>/PMS with the corresponding EELS elemental mapping image of (e) Ti and (f) S, (g) FT-IR spectra and (h) XPS sulfur binding energy (S 2p) spectra of pure TiO<sub>2</sub>, PMS, and TiO<sub>2</sub>/PMS.

Diffuse reflectance measurement demonstrates that the TiO<sub>2</sub>/PMS mixture produced a broad absorption tail that extends up to 500 nm whereas visible light absorption band did not appear at all in the spectrum of pure TiO<sub>2</sub> (Fig. 4). This implies the formation of a visible-light-absorbing surface complex involving PMS. Fig. 4 shows the photosensitizing activity of TiO<sub>2</sub>/PMS for the oxidative degradation of 4-CP and DCA under different wavelengths of visible light irradiation, which were controlled using a suite of optical filters cutting off below the specific wavelengths. The photosensitized oxidation was retarded with increasing the cut-off wavelength, with  $k(\text{DCA}) = 0.549 \text{ h}^{-1}$  under  $\lambda > 420 \text{ nm}$  and  $k(\text{DCA}) = 0.167 \text{ h}^{-1}$  under  $\lambda > 455 \text{ nm}$ , was significantly hindered under  $\lambda > 550 \text{ nm}$  and negligible under  $\lambda > 645 \text{ nm}$ . The wavelength-dependent photosensitizing activity of TiO<sub>2</sub>/PMS correlates well with its UV–visible absorption spectrum (Fig. 4), which suggests that the surface CT complex should be responsible for visible-light-induced oxidation in the TiO<sub>2</sub>/PMS suspensions.

### 3.3. Effects of reaction parameters

We monitored the 4-CP degradation kinetics in the TiO<sub>2</sub>/PMS suspensions with increasing PMS dosage (Fig. 5a). 4-CP decay was gradually accelerated as initial PMS concentration increased up to 0.5 mM above which the further increase of [PMS] was not effective. It is noteworthy that the IR peak assigned to S–O band and visible absorption band in the DRS became more intense when increasing the initial PMS concentration from 10 mM to 100 mM (Figs. 3g and 4). This reveals that the PMS level that causes the complete TiO<sub>2</sub> surface coverage through the complexation should be much higher than the PMS level (0.5–5 mM) that maximizes the photosensitizing activity of TiO<sub>2</sub>/PMS. No further kinetic enhancement in 4-CP degradation at [PMS] > 0.5 mM may be attributed to the competition between PMS and 4-CP for SO<sub>4</sub><sup>•-</sup> rather than TiO<sub>2</sub> surface saturation. PMS that is highly concentrated on TiO<sub>2</sub> surface should readily consume SO<sub>4</sub><sup>•-</sup> even if the rate constant for the oxidation of PMS by SO<sub>4</sub><sup>•-</sup> is not significant ( $k(\text{PMS} + \text{SO}_4^{\bullet-}) < 10^5 \text{ M}^{-1} \text{ s}^{-1}$ ) [36].

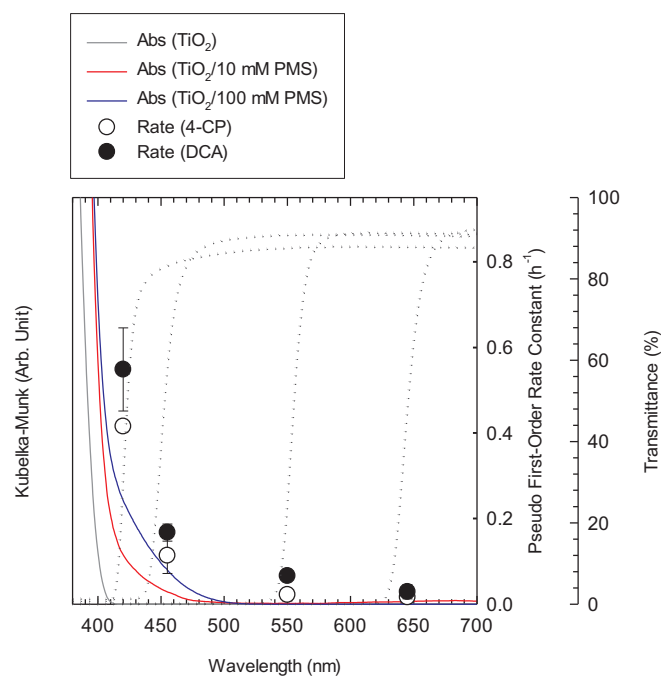


**Fig. 4.** UV-visible diffuse reflectance spectra of bare  $\text{TiO}_2$  and  $\text{TiO}_2/\text{PMS}$ , which are compared with the rate constant of the degradation of 4-CP by  $\text{TiO}_2/\text{PMS}$  as a function of the irradiation wavelengths (controlled by a set of long-pass filters transmitting  $\lambda > 420, 455, 550,$  and  $645$  nm) ( $[\text{TiO}_2]_0 = 0.5$  g/L;  $[\text{PMS}]_0 = 0.5$  mM;  $[\text{4-CP}]_0 = 100$   $\mu\text{M}$ ;  $\text{pH}_i = 5.0$ ). The dotted lines indicate the transmittance profiles of the cut-off filters.

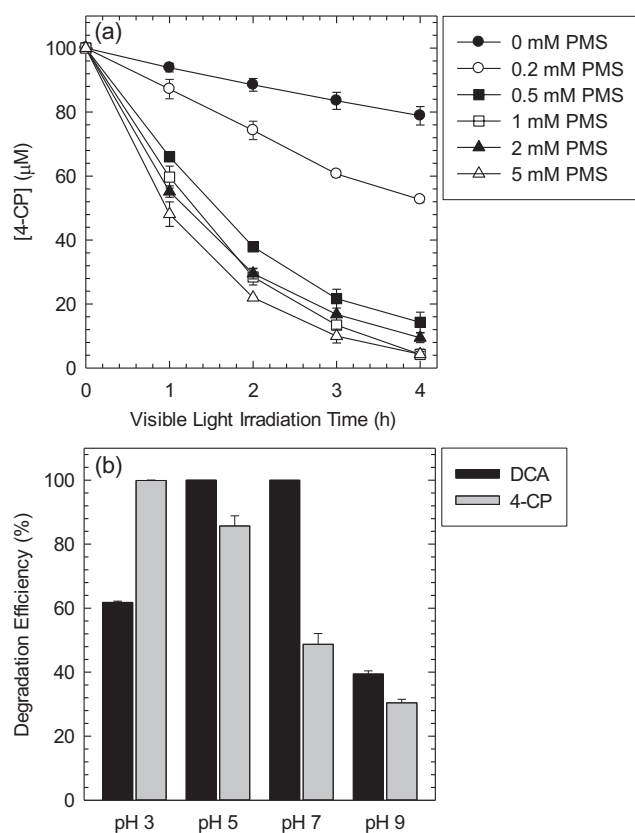


**Fig. 5.** Effects of (a) initial PMS concentration and (b) pH on the activity of  $\text{TiO}_2/\text{PMS}$  for the degradation of organic substrates ( $[\text{TiO}_2]_0 = 0.5$  g/L;  $[\text{4-CP}]_0 = [\text{DCA}]_0 = 100$   $\mu\text{M}$ ).

**Fig. 5b** shows the pH-dependent efficiencies of the  $\text{TiO}_2/\text{PMS}$  system for degradation of 4-CP and DCA. Different pH effects were observed; 4-CP oxidation decreased with increasing pH whereas weakly acidic and neutral pH condition favored DCA degradation. PMS exists as an anion over a wide pH range (i.e.,  $\text{p}K_{a1} = 0.4$  and  $\text{p}K_{a2} = 9.3$ ) [37,38], and the  $\text{TiO}_2$  surface is positively and negatively charged in acidic and basic condition, respectively (pH of the point of zero charge = 6.3) [39]. Accordingly, 4-CP and DCA decay was kinetically retarded at basic pH where surface complexation of PMS is likely inhibited due to the electrostatic repulsion between PMS and  $\text{TiO}_2$ . Since the electrostatic attraction at acidic pH facilitates the formation of the CT complex of PMS on  $\text{TiO}_2$  surface, the organic destruction is likely to be more rapid at pH 3 as observed in the case of 4-CP degradation. However, DCA oxidation was retarded at pH 3.0, which might be attributable to the competition of DCA and PMS anions for the positively-charged  $\text{TiO}_2$  surface sites.

### 3.4. Effects of anions

**Fig. 1** showed no visible light activity of P- $\text{TiO}_2/\text{PMS}$  for oxidative degradation of 4-CP, which was presumably due to the inhibitory effect of surface-bound phosphate on the formation of  $\text{TiO}_2$ -PMS CT complex. To further identify the role of phosphate as a protective agent, surface chemical composition of P- $\text{TiO}_2$  after exposure to excess PMS was analyzed; no appearance of the FT-IR band assignable to surface S-O group (**Fig. S6a**) and no detection of sulfur element on P- $\text{TiO}_2$  in the EELS image (**Fig. S6j**) indicate the inability of P- $\text{TiO}_2$  to form the surface complex with PMS. UV-visible diffuse reflectance spectrum of P- $\text{TiO}_2/\text{PMS}$  ensured that PMS addition did not extend the absorption of P- $\text{TiO}_2$  into visible light region (**Fig. S6b**). A comparison among different anion-modified  $\text{TiO}_2$  samples (i.e., fluoride, iodate, sulfate, perchlorate, and phosphate) were prepared according to the procedure described in the Section 2.2) for the PMS adsorption capacity showed that P- $\text{TiO}_2$  barely removed PMS via sorption mechanism whereas other anion-modified  $\text{TiO}_2$  caused a noticeable sorption of PMS concentration in the dark (**Fig. S7**). This corroborated that surface-adsorbed phosphates effectively hindered PMS sorption and its surface complexation on  $\text{TiO}_2$ . The influence of naturally-occurring anions (i.e.,  $\text{Cl}^-$ , sulfate ( $\text{SO}_4^{2-}$ ), and bicarbonate ( $\text{HCO}_3^-$ )) on the LMCT-mediated oxidation on  $\text{TiO}_2/\text{PMS}$  was also investigated by monitoring 4-CP degradation kinetics in the presence of each anion. Regardless of the anion type, 4-CP decomposition by  $\text{TiO}_2/\text{PMS}$  was not kinetically retarded in the presence of 1 mM anions ( $\text{Cl}^-$ ,  $\text{SO}_4^{2-}$ , and  $\text{HCO}_3^-$ , respectively), which likely rules out the possibility of competition between background anions and PMS for surface complexation sites on  $\text{TiO}_2$  (data not shown).

### 3.5. Role of $\text{SO}_4^{\cdot-}$ as the main oxidant

To identify the primary degradative pathway induced by visible-light-irradiated  $\text{TiO}_2/\text{PMS}$ , the effects of two radical quenchers, methanol (MeOH) and *tert*-butyl alcohol (*t*-BuOH) were explored (**Fig. 6a**). The addition of excess MeOH completely inhibited DCA degradation and markedly retarded the degradation of 4-CP. These results suggest the involvement of  $\text{SO}_4^{\cdot-}$  in oxidative degradation associated with the CT complex-mediated PMS activation. 4-CP was still degraded to a certain extent even in the presence of excess MeOH, which implies the alternative reaction route involving no  $\text{SO}_4^{\cdot-}$ ;  $\text{TiO}_2$ -4CP CT complexes mediated the self-sensitized degradation of 4-CP (i.e.,  $(\text{TiO}_2\text{-4CP complex})^* \rightarrow 4\text{-CP}^{\cdot+} + \text{TiO}_2(e^-)$ ). Note that one-electron oxidation via the LMCT mechanism is kinetically enhanced in the presence of electron acceptors such as PMS and Cr(VI) (**Fig. S8**). The apparent quenching effect of *t*-BuOH may raise the possibility of  $\cdot\text{OH}$ -induced oxidation since *t*-BuOH reacts selectively with  $\cdot\text{OH}$  ( $k(t\text{-BuOH} + \cdot\text{OH}) = 3.8 \times 10^8 \text{ M}^{-1} \text{ s}^{-1}$  versus  $k(t\text{-BuOH} + \text{SO}_4^{\cdot-}) = 4 \times 10^5 \text{ M}^{-1} \text{ s}^{-1}$ ) [40]. However, this is likely attributed to the competition between PMS and *t*-BuOH for sorption sites onto  $\text{TiO}_2$ ; PMS degradation efficiency in the  $\text{TiO}_2/\text{PMS}$  suspension was

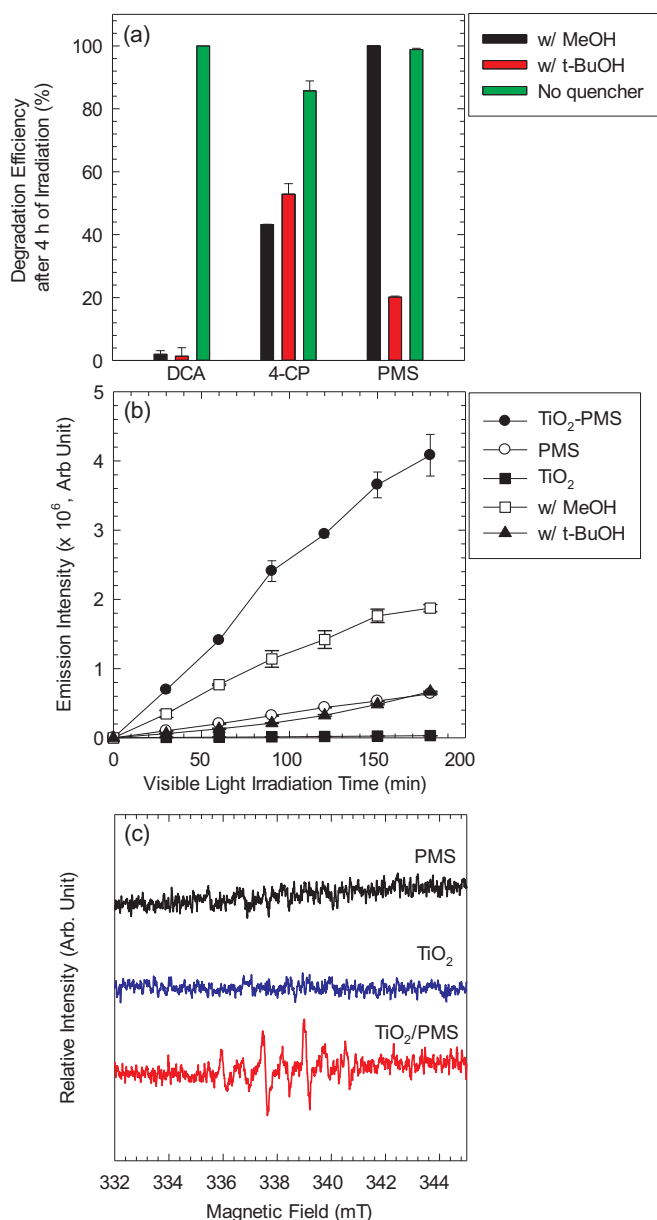


**Fig. 6.** (a) Effects of quenchers on the activity of TiO<sub>2</sub>/PMS for the degradation of organic substrate and PMS, (b) visible light-induced production of hydroxylated coumarin (monitored by its fluorescence emission) in the suspension of pure TiO<sub>2</sub>, PMS, and TiO<sub>2</sub>/PMS, and (c) DMPO spin trap EPR spectra measured in the visible light-irradiated suspension of pure TiO<sub>2</sub>, PMS, and TiO<sub>2</sub>/PMS ([TiO<sub>2</sub>]<sub>0</sub> = 0.5 g/L; [PMS]<sub>0</sub> = 0.5 mM; [4-CP]<sub>0</sub> = [DCA]<sub>0</sub> = 100 μM, [MeOH]<sub>0</sub> = [t-BuOH]<sub>0</sub> = 100 mM; [DMPO]<sub>0</sub> = 90 mM; pH<sub>i</sub> = 5.0).

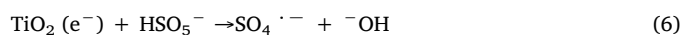
not reduced at all in the presence of MeOH whereas PMS decomposition was significantly decelerated upon *t*-BuOH addition (Fig. 6a).

To further confirm the role of SO<sub>4</sub><sup>•-</sup> in the TiO<sub>2</sub>/PMS system, we monitored the hydroxylation of coumarin as an indirect indicator for radical production in the visible-light-irradiated TiO<sub>2</sub>/PMS (Fig. 6b), which is based on the findings that the attack of SO<sub>4</sub><sup>•-</sup> on aromatics led to the formation of hydroxylated compounds as the major products [41]. Note that the similarity in the distribution of transient intermediates during coumarin oxidation allows us to use <sup>•</sup>OH measurement methods for quantitatively monitoring SO<sub>4</sub><sup>•-</sup> [42,43]. Whereas the formation of 7-hydroxycoumarin was almost absent with PMS or TiO<sub>2</sub> alone, the hydroxylated product concentration linearly increased with the irradiation time in the TiO<sub>2</sub>/PMS suspension. The coumarin hydroxylation considerably decreased in the presence of MeOH as a

SO<sub>4</sub><sup>•-</sup> scavenger. In particular, it is interesting to note that the retarding effect was more pronounced with *t*-BuOH that is a poor scavenger of SO<sub>4</sub><sup>•-</sup> [7,44,45]. This seems to imply that the presence of *t*-BuOH hinders the adsorption of PMS on TiO<sub>2</sub> sites. Furthermore, DMPO-SO<sub>4</sub><sup>•-</sup> adduct was detected only in the EPR spectrum of TiO<sub>2</sub>/PMS whereas neither PMS nor TiO<sub>2</sub> alone produced the peak pattern characteristic of SO<sub>4</sub><sup>•-</sup> in the presence of DMPO as a spin-trapping agent (Fig. 6c). It is clear that the generation of SO<sub>4</sub><sup>•-</sup> should be induced by the photoexcitation of the surface complex of PMS on TiO<sub>2</sub>.

### 3.6. Activation mechanisms and processes

According to some spectroscopic evidences (Figs. 3g, h, and 4), PMS adsorption is likely to produce a visible-light-absorbing complex at TiO<sub>2</sub> surface (i.e., >Ti-OH + HSO<sub>5</sub><sup>-</sup> → >Ti-OOSO<sub>3</sub><sup>-</sup> + H<sub>2</sub>O). The visible-light-induced LMCT leads to electron injection into the CB of TiO<sub>2</sub> (Eq. (5)).



A direct evidence for the visible light-induced LMCT was obtained by comparing the photocurrent generated on TiO<sub>2</sub> electrode under visible light with and without PMS. PMS addition induced a significant current generation at TiO<sub>2</sub> electrode under visible light irradiation, but little photocurrent generation was observed in the absence of PMS (Fig. 7). This confirmed the direct electron transfer from the visible-light-excited surface complex (PMS/TiO<sub>2</sub>) to the CB of TiO<sub>2</sub>. In this event, PMS coordinated to the Ti-surface site acts as an electron donor and another PMS readily undergoes reductive conversion into SO<sub>4</sub><sup>•-</sup> by electrons transferred via LMCT (Eq. (6)). Phenolic compounds that form CT complexes at TiO<sub>2</sub> surface may provide an additional reaction pathway for one-electron reduction of PMS. However, the effective degradation of organic substrates (e.g., DCA, carbamazepine) still proceeds on TiO<sub>2</sub> in the presence of PMS even though their roles as complexing agents are not significant, which assures that twofold actions of PMS as a ligand of the CT complexation and as a precursor of SO<sub>4</sub><sup>•-</sup> are critical in the visible-light-sensitized oxidation of organics. PMS radical (SO<sub>5</sub><sup>•-</sup>) may form during LMCT subsequent to the excitation of the interfacial CT complex. Based on the previous finding that the recombination of SO<sub>5</sub><sup>•-</sup> caused rapid SO<sub>4</sub><sup>•-</sup> generation (i.e., SO<sub>5</sub><sup>•-</sup> + SO<sub>5</sub><sup>•-</sup> → SO<sub>4</sub><sup>•-</sup> + SO<sub>4</sub><sup>•-</sup> + O<sub>2</sub>; *k* = 2.2 × 10<sup>8</sup> M<sup>-1</sup> s<sup>-1</sup>) [36], this collateral reaction route would contribute to the overall efficiency of SO<sub>4</sub><sup>•-</sup> production.

We compared TiO<sub>2</sub>/PMS/visible light versus Co<sub>3</sub>O<sub>4</sub>/PMS (a

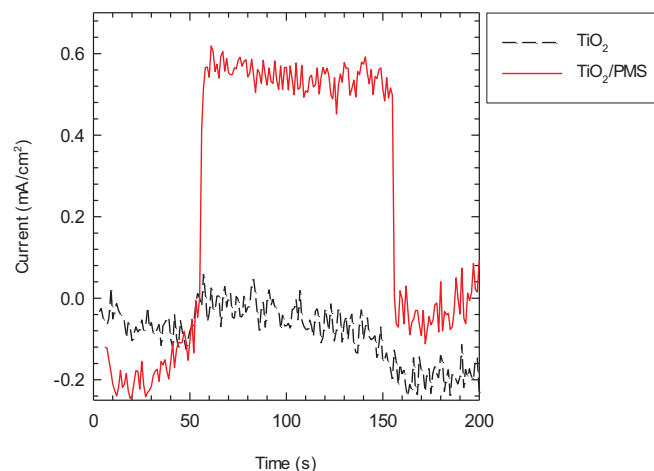


**Fig. 7.** Photocurrent generation at TiO<sub>2</sub> electrode in the absence and presence of PMS ([PMS]<sub>0</sub> = 0.5 mM; [LiClO<sub>4</sub>]<sub>0</sub> = 10 mM; pH<sub>i</sub> = 5.0).

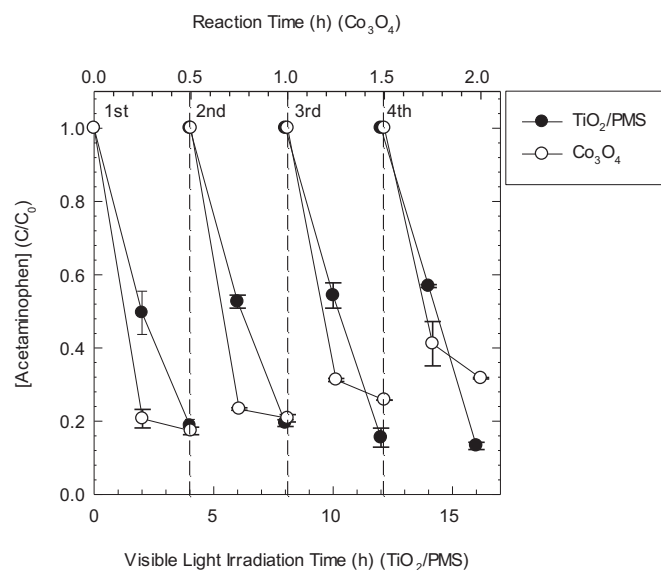


**Fig. 8.** Repeated degradation of acetaminophen by Co<sub>3</sub>O<sub>4</sub> and visible-light-irradiated TiO<sub>2</sub>/PMS ([TiO<sub>2</sub>]<sub>0</sub> = [Co<sub>3</sub>O<sub>4</sub>]<sub>0</sub> = 0.5 g/L; [PMS]<sub>0</sub> = 0.5 mM; [acetaminophen]<sub>0</sub> = 100 μM; pH<sub>i</sub> = 5.0).

benchmark system to produce SO<sub>4</sub><sup>•−</sup> in the dark) in terms of the repeated oxidation of acetaminophen (Fig. 8). Catalytic performance of activators (*i.e.*, TiO<sub>2</sub> and Co<sub>3</sub>O<sub>4</sub>) was examined in the same batch with fresh PMS supplied in each cycle. The use of Co<sub>3</sub>O<sub>4</sub> as a PMS activator led to gradual reduction in organic degradation efficiency. In contrast, TiO<sub>2</sub>/PMS exhibited constant activity for acetaminophen oxidation over multiple cycles. In persulfate activation processes utilizing metals and metal oxides, the electron exchange between persulfate and metal-based activators results in SO<sub>4</sub><sup>•−</sup> production, which should be accompanied by the oxidative transformation of the activator itself. This likely causes a loss of PMS activating capacity of Co<sub>3</sub>O<sub>4</sub> during the repeated uses. In contrast, TiO<sub>2</sub> that provides a metallic coordination center in the LMCT mechanism remains intact in the catalytic cycles since electrons to activate PMS originate from PMS itself bound to the surface of TiO<sub>2</sub>.

#### 4. Conclusions

This study demonstrated the first instance of visible-light-induced oxidation of organic pollutants via a TiO<sub>2</sub>-PMS CT complex. Unlike the conventional photochemical activation methods to excite either PMS or TiO<sub>2</sub> with UV light, the dual roles of PMS as a surface complexing ligand and a radical precursor allow visible light (or natural sunlight) to activate PMS on TiO<sub>2</sub>. Several spectroscopic analyses confirmed the surface complexation of TiO<sub>2</sub> with PMS through the condensation reaction, and the absorption spectrum of TiO<sub>2</sub>/PMS in the visible light region is consistent with the wavelength-dependent degradation of 4-CP. Visible-light-driven production of SO<sub>4</sub><sup>•−</sup> was supported by the following results: significant quenching effect of methanol, effective coumarin hydroxylation, EPR spectral features corresponding to the radical adduct, and substrate-specific treatment efficiency that matched the reactivity of SO<sub>4</sub><sup>•−</sup>. Since the net reaction for PMS activation on TiO<sub>2</sub> is electron exchange between two PMS molecules (*i.e.*, electron transfer from PMS as a complexing agent to another PMS as a SO<sub>4</sub><sup>•−</sup> precursor: Eq. (5) + Eq. (6)), the oxidative degradation of organic pollutants can repeatedly proceed on TiO<sub>2</sub> as long as persulfate is sufficiently supplied. The persulfate activation on TiO<sub>2</sub> via LMCT is advantageous since it needs low photon energy and durable and low-cost catalyst.

#### Acknowledgements

This work was financially supported by the Global Research Laboratory (GRL) Program (No. NRF-2014K1A1A2041044), Basic Science Research Program (NRF-2017R1A2B2008952), KCAP (Sogang Univ.) (No. 2009-0093880), and Basic Science Research Program (2017R1A2B4002235), which were funded by the Korea Government (MSIP) through the National Research Foundation of Korea (NRF).

#### Appendix A. Supplementary data

Supplementary data associated with this article can be found, in the online version, at <http://dx.doi.org/10.1016/j.cej.2018.03.150>.

#### References

- [1] P. Neta, R.E. Huie, A.B. Ross, Rate constants for reactions of inorganic radicals in aqueous solution, *J. Phys. Chem. Ref. Data* 17 (1988) 1027–1284.
- [2] A. Tsitonaki, B. Petri, M. Crimi, H. Mosbaek, R.L. Siegrist, P.L. Bjerg, In situ chemical oxidation of contaminated soil and groundwater using persulfate: a review, *Crit. Rev. Environ. Sci. Technol.* 40 (2010) 55–91.
- [3] S. Wacławek, H.V. Lutze, K. Grübel, V.V.T. Padil, M. Černík, D.D. Dionysiou, Chemistry of persulfates in water and wastewater treatment: a review, *Chem. Eng. J.* 330 (2017) 44–62.
- [4] G.V. Buxton, C.L. Greenstock, W.P. Helman, A.B. Ross, Critical review of rate constants for reactions of hydrated electrons, hydrogen atoms and hydroxyl radicals (OH<sup>•</sup>/O<sup>•</sup>) in Aqueous-Solution, *J. Phys. Chem. Ref. Data* 17 (1988) 513–886.
- [5] Y.C. Lee, S.L. Lo, P.T. Chiueh, D.G. Chang, Efficient decomposition of perfluorocarboxylic acids in aqueous solution using microwave-induced persulfate, *Water Res.* 43 (2009) 2811–2816.
- [6] P. Manoj, R. Varghese, V.M. Manoj, C.T. Aravindakumar, Reaction of sulphate radical anion (SO<sub>4</sub><sup>•−</sup>) with cyanuric acid: A potential reaction for its degradation? *Chem. Lett.* 74–75 (2002).
- [7] G.P. Anipsitakis, D.D. Dionysiou, Degradation of organic contaminants in water with sulfate radicals generated by the conjunction of peroxymonosulfate with cobalt, *Environ. Sci. Technol.* 37 (2003) 4790–4797.
- [8] G.P. Anipsitakis, D.D. Dionysiou, Transition metal/UV-based advanced oxidation technologies for water decontamination, *Appl. Catal., B* 54 (2004) 155–163.
- [9] K. Govindan, M. Raja, S.U. Maheshwari, M. Noel, Analysis and understanding of amido black 10B dye degradation in aqueous solution by electrocoagulation with the conventional oxidants peroxymonosulfate, peroxodisulfate and hydrogen peroxide, *Environ. Sci.: Water Res.* 1 (2015) 108–119.
- [10] K. Govindan, M. Raja, M. Noel, E.J. James, Degradation of pentachlorophenol by hydroxyl radicals and sulfate radicals using electrochemical activation of peroxymonosulfate, peroxodisulfate and hydrogen peroxide, *J. Hazard. Mater.* 272 (2014) 42–51.
- [11] J. Criquet, N.K.V. Leitner, Electron beam irradiation of aqueous solution of persulfate ions, *Chem. Eng. J.* 169 (2011) 258–262.
- [12] W.S. Chen, Y.C. Su, Removal of dinitrotoluenes in wastewater by sono-activated persulfate, *Ultrason. Sonochem.* 19 (2012) 921–927.
- [13] W.S. Chen, C.P. Huang, Mineralization of aniline in aqueous solution by electrochemical activation of persulfate, *Chemosphere* 125 (2015) 175–181.
- [14] A. Ghauch, A.M. Tuqan, N. Kibbi, Ibuprofen removal by heated persulfate in aqueous solution: a kinetics study, *Chem. Eng. J.* 197 (2012) 483–492.
- [15] Y.C. Chou, S.L. Lo, J. Kuo, C.J. Yeh, Microwave-enhanced persulfate oxidation to treat mature landfill leachate, *J. Hazard. Mater.* 284 (2015) 83–91.
- [16] Y.J. Qian, X. Guo, Y.L. Zhang, Y. Peng, P.Z. Sun, C.H. Huang, J.F. Niu, X.F. Zhou, J.C. Crittenden, Perfluorooctanoic acid degradation Using UV-persulfate process: modeling of the degradation and chlorate formation, *Environ. Sci. Technol.* 50 (2016) 772–781.
- [17] X.Y. Chen, W.P. Wang, H. Xiao, C.L. Hong, F.X. Zhu, Y.L. Yao, Z.Y. Xue, Accelerated TiO<sub>2</sub> photocatalytic degradation of Acid Orange 7 under visible light mediated by peroxymonosulfate, *Chem. Eng. J.* 193 (2012) 290–295.
- [18] Y.F. Tao, Q. Ni, M.Y. Wei, D.S. Xia, X.X. Li, A.H. Xu, Metal-free activation of peroxymonosulfate by g-C<sub>3</sub>N<sub>4</sub> under visible light irradiation for the degradation of organic dyes, *RSC Adv.* 5 (2015) 44128–44136.
- [19] S. Kim, W. Choi, Visible-light-induced photocatalytic degradation of 4-chlorophenol and phenolic compounds in aqueous suspension of pure titania: demonstrating the existence of a surface-complex-mediated path, *J. Phys. Chem. B* 109 (2005) 5143–5149.
- [20] G. Kim, W. Choi, Charge-transfer surface complex of EDTA-TiO<sub>2</sub> and its effect on photocatalysis under visible light, *Appl. Catal., B* 100 (2010) 77–83.
- [21] Y. Park, N.J. Singh, K.S. Kim, T. Tachikawa, T. Majima, W. Choi, Fullerol-titania charge-transfer-mediated photocatalysis working under visible light, *Chem. Eur. J.* 15 (2009) 10843–10850.
- [22] G. Kim, S.H. Lee, W. Choi, Glucose-TiO<sub>2</sub> charge transfer complex-mediated photocatalysis under visible light, *Appl. Catal., B* 162 (2015) 463–469.
- [23] G. Zhang, G. Kim, W. Choi, Visible light driven photocatalysis mediated via ligand-to-metal charge transfer (LMCT): an alternative approach to solar activation of titania, *Energy Environ. Sci.* 7 (2014) 954–966.
- [24] T. Ohno, Y. Masaki, S. Hirayama, M. Matsumura, TiO<sub>2</sub>-photocatalyzed epoxidation

- of 1-decene by  $\text{H}_2\text{O}_2$  under visible light, *J. Catal.* 204 (2001) 163–168.
- [25] X.Z. Li, C.C. Chen, J.C. Zhao, Mechanism of photodecomposition of  $\text{H}_2\text{O}_2$  on  $\text{TiO}_2$  surfaces under visible light irradiation, *Langmuir* 17 (2001) 4118–4122.
- [26] Y.R. Wang, J. Le Roux, T. Zhang, J.P. Croue, Formation of brominated disinfection byproducts from natural organic matter isolates and model compounds in a sulfate radical-based oxidation process, *Environ. Sci. Technol.* 48 (2014) 14534–14542.
- [27] G. Louit, S. Foley, J. Cabillic, H. Coffigny, F. Taran, A. Valleix, J.P. Renault, S. Pin, The reaction of coumarin with the OH radical revisited: hydroxylation product analysis determined by fluorescence and chromatography, *Radiat. Phys. Chem.* 72 (2005) 119–124.
- [28] J. Lim, A.D. Bokare, W. Choi, Visible light sensitization of  $\text{TiO}_2$  nanoparticles by a dietary pigment, curcumin, for environmental photochemical transformations, *RSC Adv.* 7 (2017) 32488–32495.
- [29] G.R. Peyton, The free-radical chemistry of persulfate-based total organic carbon analyzers, *Mar. Chem.* 41 (1993) 91–103.
- [30] P.A. Connor, A.J. McQuillan, Phosphate adsorption onto  $\text{TiO}_2$  from aqueous solutions: an in situ internal reflection infrared spectroscopic study, *Langmuir* 15 (1999) 2916–2921.
- [31] P. Neta, V. Madhavan, H. Zemel, R.W. Fessenden, Rate constants and mechanism of reaction of  $\text{SO}_4^{\cdot-}$  with aromatic compounds, *J. Am. Chem. Soc.* 99 (1977) 163–164.
- [32] J. Deng, Y.S. Shao, N.Y. Gao, Y. Deng, S.Q. Zhou, X.H. Hu, Thermally activated persulfate (TAP) oxidation of antiepileptic drug carbamazepine in water, *Chem. Eng. J.* 228 (2013) 765–771.
- [33] J. Deng, Y.S. Shao, N.Y. Gao, S.J. Xia, C.Q. Tan, S.Q. Zhou, X.H. Hu, Degradation of the antiepileptic drug carbamazepine upon different UV-based advanced oxidation processes in water, *Chem. Eng. J.* 222 (2013) 150–158.
- [34] J. Gonzalez, M. Torrent-Sucarrat, J.M. Anglada, The reactions of  $\text{SO}_3$  with  $\text{HO}_2$  radical and  $\text{H}_2\text{O}-\text{HO}_2$  radical complex. Theoretical study on the atmospheric formation of  $\text{HSO}_5$  and  $\text{H}_2\text{SO}_4$ , *Phys. Chem. Chem. Phys.* 12 (2010) 2116–2125.
- [35] Y.J. He, J.F. Peng, W. Chu, Y.Z. Li, D.G. Tong, Black mesoporous anatase  $\text{TiO}_2$  nanoleaves: a high capacity and high rate anode for aqueous Al-ion batteries, *J. Mater. Chem. A* 2 (2014) 1721–1731.
- [36] T.N. Das, Reactivity and role of  $\text{SO}_5^{\cdot-}$  radical in aqueous medium chain oxidation of sulfite to sulfate and atmospheric sulfuric acid generation, *J. Phys. Chem. A* 105 (2001) 9142–9155.
- [37] H. Elias, U. Gotz, K.J. Wannowius, Kinetics and mechanism of the oxidation of sulfur(IV) by peroxomonosulfuric acid anion, *Atmos. Environ.* 28 (1994) 439–448.
- [38] D.F. Evans, M.W. Upton, Studies on singlet oxygen in aqueous solution 3. The decomposition of peroxy acids, *J. Chem. Soc. Dalton Trans.* (1985) 1151–1153.
- [39] M.M. Halmann, *Photodegradation of Water Pollutants*, CRC Press, New York, USA, 1996.
- [40] G.P. Anipsitakis, D.D. Dionysiou, Radical generation by the interaction of transition metals with common oxidants, *Environ. Sci. Technol.* 38 (2004) 3705–3712.
- [41] George P. Anipsitakis, Dionysios D. Dionysiou, M.A. Gonzalez, Cobalt-mediated activation of peroxymonosulfate and sulfate radical attack on phenolic compounds: Implications of chloride ions, *Environ. Sci. Technol.* 40 (2006) 1000–1007.
- [42] Wen-Da Oh, Zhili Dong, T.-T. Lim, Generation of sulfate radical through heterogeneous catalysis for organic contaminants removal: current development, challenges and prospects, *Appl. Catal., B* 194 (2016) 169–201.
- [43] T.S. Singh, B.S.M. Rao, H. Mohan, J.P. Mittal, A pulse radiolysis of coumarin and its derivatives, *J. Photochem. Photobiol., A* 153 (2002) 163–171.
- [44] R. Li, J. Kong, H. Liu, P. Chen, G. Liu, F. Li, W. Lv, A sulfate radical based ferrous-peroxydisulfate oxidative system for indomethacin degradation in aqueous solutions, *RSC Adv.* (2017) 22802–22809.
- [45] F. Qi, W. Chu, B. Xu, Catalytic degradation of caffeine in aqueous solutions by cobalt-MCM41 activation of peroxymonosulfate, *Appl. Catal., B* 134–135 (2013) 324–332.